

## Critical-current suppression in sub-micron intrinsic Josephson junction arrays

This article has been downloaded from IOPscience. Please scroll down to see the full text article.

2006 J. Phys.: Conf. Ser. 43 1114

(<http://iopscience.iop.org/1742-6596/43/1/271>)

View [the table of contents for this issue](#), or go to the [journal homepage](#) for more

Download details:

IP Address: 144.82.107.49

The article was downloaded on 16/08/2013 at 16:22

Please note that [terms and conditions apply](#).

# Critical-current suppression in sub-micron intrinsic Josephson junction arrays

J C Fenton<sup>1,2</sup>, M Korsah<sup>3</sup>, C R M Grovenor<sup>3</sup> and P A Warburton<sup>1,2</sup>

<sup>1</sup>University College London, Department of Electrical and Electronic Engineering, Torrington Place, London WC1E 7JE, UK

<sup>2</sup>London Centre for Nanotechnology, 17–19 Gordon Street, London WC1H 0AH, UK

<sup>3</sup>University of Oxford, Department of Materials, Oxford, OX1 3PH, UK

E-mail: j.fenton@ee.ucl.ac.uk, p.warburton@ee.ucl.ac.uk

**Abstract.** We present experimental results on intrinsic Josephson junctions fabricated by three-dimensional gallium focussed-ion-beam (FIB) milling in *c*-axis-oriented  $\text{Tl}_2\text{Ba}_2\text{CaCu}_2\text{O}_8$  thin films. We report measurements of the dependence of the switching current density of these arrays at 4.2 K upon the junction cross-sectional area  $A$  showing strong suppression of the switching current density for junctions with  $A \lesssim 1 \mu\text{m}^2$ ; the switching current extrapolates to zero for  $A \sim 0.25 \mu\text{m}^2$ . We discuss the roles of gallium ion implantation and both thermal and quantum fluctuations in this current suppression. We also present *in-situ*  $IV$  measurements demonstrating the use of a liquid-helium-cooled sample stage in conjunction with the FIB milling.

## 1. Introduction

The spacing of consecutive copper-oxide double planes in the most anisotropic cuprate superconductors is greater than the coherence length in the out-of-plane *c*-direction. When a current flows along the *c*-direction in such a material, it therefore flows through a series array of “intrinsic” Josephson junctions (IJJs) [1]. These junctions and junction arrays are showing promise for a wide variety of applications, including as voltage standards and sub-mm-wave oscillators [2]. For sub-micron intrinsic junctions, there is an additional range of potential applications exploiting the Coulomb blockade effect, when the charging energy  $E_C \gtrsim E_J, kT$ , where  $E_J$  is the Josephson energy. These applications include electric-field sensors and quantum current standards [3]. In long arrays of junctions,  $E_C$  is enhanced by electron-electron interactions [4, 5] by a factor  $\sqrt{C/C_0}$ , where  $C$  is the junction capacitance and  $C_0$  is the stray capacitance to ground. The large ratio  $C/C_0 \sim 10^6$  for intrinsic junctions makes them particularly suited to applications involving Coulomb blockade effects.

We fabricate IJJ arrays with cross-sectional area  $A \lesssim 1 \mu\text{m}^2$  using three-dimensional focussed ion-beam (FIB) milling [6, 7] of  $\text{Tl}_2\text{Ba}_2\text{CaCu}_2\text{O}_8$  (TBCCO) thin films on lanthanum aluminate substrates. Our devices show high-quality underdamped (Stewart–McCumber parameter  $\beta_c > 10^3$ ) current-voltage ( $IV$ ) characteristics comparable to those obtained on single crystals. Here we report strong suppression of the apparent critical current for junctions with  $A < 1 \mu\text{m}^2$ , which may be the result of quantum fluctuations.

While our FIB fabrication process already gives us the ability to make sub- $\mu\text{m}^2$  junctions, our system also includes the option of a liquid-helium-cooled sample stage with the capability

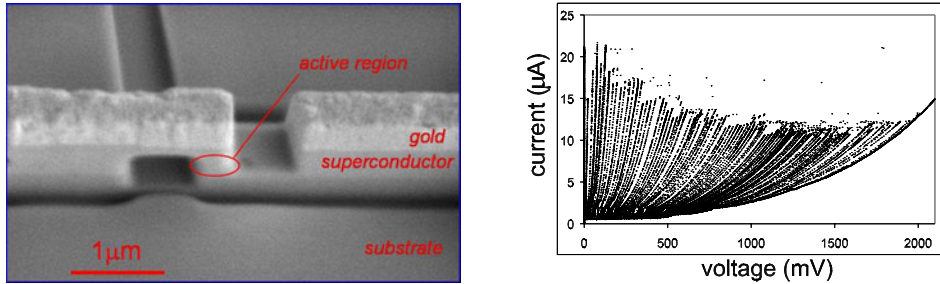


**Figure 1.** (a) Scanning electron micrograph showing the side view of a completed TBCCO intrinsic junction stack. (b) Four-point  $IV$  characteristics of an intrinsic junction stack with  $A = 0.7 \mu\text{m}^2$  at 4.2 K.

for *in-situ*  $IV$  measurements. This allows real-time monitoring of the  $IV$  characteristics during milling. We also present  $IV$  data obtained *in situ* using the liquid-helium-cooled sample stage during FIB narrowing of a junction array.

## 2. Experimental

Our devices are fabricated from  $c$ -axis-oriented TBCCO films [7]. A completed device is shown in Fig. 1(a). The geometry is based on a similar device fabricated in Bi-Sr-Ca-Cu-O whiskers by S.J. Kim *et al.* [6]. Optical lithography and argon ion-milling are used to pattern tracks which connect the junction arrays to large pads at the edge of the sample. Tracks of width  $w$  (typically  $0.7 \mu\text{m}$ ) are patterned in the film using normally-incident FIB milling with a 30-keV gallium ion beam. The substrate is then rotated so that the ion beam is almost parallel to it. Slots separated by distance  $y$  are then milled laterally through the track, as shown in Fig. 1(a). These force the current to flow parallel to the  $c$ -axis in the central part of the structure, creating a stack of intrinsic junctions with  $A = wy$  and stack height  $z$ , containing  $N$  intrinsic junctions, where we expect  $N = (z/1.7 \text{ nm})$ .

After fabrication, four-point current-sourced measurements of the electronic properties of the devices may be performed in a liquid-helium storage vessel. Micro-coaxial cables and room-temperature low-pass filters are used to reduce external noise.

We also have the capability to mount samples in the FIB microscope on a dedicated liquid-helium-cooled sample stage. This sample stage is based on a copper block wrapped with tubes through which liquid helium is pumped from a storage dewar in continuous-flow configuration. The base temperature at the sample is below 20 K and stage drift at base temperature is  $\lesssim 50 \text{ nm/min}$ . Eight wires are attached to the sample stage, so electrical measurements in four-point configuration are possible. Samples may be FIB milled at normal incidence while the device  $IV$  characteristics are monitored *in situ*. Noise from the beam scan-generators is noticeable, although smaller than the signals we are measuring. Because the beam current is typically  $\sim 10 \text{ pA}$ ,  $IV$  measurements during milling are not affected by the beam current. This is in contrast to the case for broad-beam ion milling [8].

## 3. Results and discussion

All our devices show multi-branched  $IV$  characteristics. A good example is shown in Fig. 1(b). Since, in our sub-micron devices, dissipation occurs for  $I < I_C$ , the critical current, [9] we work with an experimentally measured quantity  $I_{\text{SW}}$ , which we define as the value of a quasi-static increasing current bias ramp at which the junction switches from the supercurrent branch to the first quasiparticle branch. The dependence on  $A$  of both  $I_{\text{SW}}$  and the switching current density

$J_{\text{SW}} = I_{\text{SW}}/A$  at  $T=4.2$  K is shown in Fig. 1(b). For  $A > 1 \mu\text{m}^2$ ,  $J_{\text{SW}}$  is independent of  $A$  as expected,  $\approx 10^4 \text{ Acm}^{-2}$ . This we take to be the unfluctuated value of the critical current density,  $J_{\text{C}}$ , in our intrinsic junctions. For sub-micron junctions, however, the switching current is suppressed, and extrapolates to zero at  $A = 0.25 \mu\text{m}^2$ .

We now briefly discuss three mechanisms for the suppression of the switching current in sub-micron intrinsic junctions: gallium ion implantation, thermal fluctuations and quantum fluctuations. A more detailed discussion is given elsewhere [10]. During focussed ion-beam milling, gallium ions are implanted into all four sidewalls of our junction stack up to some distance  $d_{\text{imp}}$ . Assuming no contribution at all to conduction from these implanted regions, the conductivity should reduce to zero at  $2d_{\text{imp}} = \min(w, y)$ . In Ref. [10], we used gallium ion-milling to sequentially reduce the width of a TBCCO thin-film track. We observed a linear decrease in the room-temperature conductance and inferred that  $d_{\text{imp}} = 90 \text{ nm}$ . This gives  $I_{\text{C}} = 0$  for a square junction when  $A < 0.032 \mu\text{m}^2$ , an order of magnitude less than the intercept  $A(I_{\text{SW}} = 0)$  in the inset of Fig. 2(a). This suggests that gallium implantation does not account fully for the switching current suppression we observe.

Thermal fluctuations can cause premature switching from the supercurrent state to the quasiparticle branch, even when  $E_{\text{J}} > kT$  (where  $E_{\text{J}} = \Phi_0 J_{\text{C}} A / 2\pi$  and  $\Phi_0$  is the flux quantum) [11, 12]. We have previously presented elsewhere a detailed study of the role of thermal fluctuations on a sub-micron device of area  $0.35 \mu\text{m}^2$  [9]. By assuming thermally-activated switching we inferred the  $I_{\text{C}} = 1.3I_{\text{SW}}(4.2 \text{ K})$  and  $J_{\text{C}} = 2.1 \times 10^3 \text{ Acm}^{-2}$ . Taking into account the reduction in effective junction area caused by gallium implantation,  $J_{\text{C}} = 3.2 \times 10^3 \text{ Acm}^{-2}$ , still significantly smaller than for our larger junctions. Thermal fluctuations and gallium implantation therefore do not appear to be the sole mechanisms for critical current suppression.

Quantum fluctuations in the phase difference across a *single* Josephson junction become significant when  $\alpha \equiv E_{\text{J}}/E_{\text{C}} \lesssim 1$ . Here  $E_{\text{C}} = (2e)^2/(2C)$  is the Coulomb energy for Cooper pairs and  $e$  is the electronic charge. Taking  $J_{\text{C}} = 10^4 \text{ Acm}^{-2}$ ,  $d = 1.4 \text{ nm}$  and  $\epsilon_{\text{r}} = 10$ , we obtain a condition  $A \lesssim 0.005 \mu\text{m}^2$  for quantum fluctuations to become important in a *single* junction. In arrays of junctions, the charging energy is enhanced due to inter-junction Coulomb interactions. In a large array, a charge ‘‘soliton’’ extending over  $\sqrt{C/C_0}$  junctions is formed and the charging energy is enhanced by the same factor [4, 5]. In a finite array of  $N$  junctions, the soliton length is clearly limited to  $N$  junctions, so the charging energy is enhanced by a factor  $\min(N, \sqrt{C/C_0})$  [13]. With  $N \sim 10^2$ , quantum fluctuations then become important around  $A \sim 0.5 \mu\text{m}^2$ .

*In-situ* monitoring of low- $T$   $IV$  characteristics during FIB milling provides an additional degree of control over the dimensions of a junction stack. Figs. 2(b) and 3 show low- $T$  two-point  $IV$  characteristics of a track before and after successive narrowing of the track by milling the low- $T$  sample. Before narrowing, the track was not laterally milled to create the slots, because the  $IV$  characteristics showed that the track already contained an array of small-area IJJs. This array is likely to have arisen due to a fortuitous configuration of film defects in the track. The dimensions of these IJJs are not well known, but we estimate  $A \approx 0.3 \mu\text{m}^2$  for most of the junctions by comparison of  $I_{\text{SW}}$  before milling with Fig. 2(a). The first switching current is reduced by successive narrowing of the track to an immeasurably small value after the final milling stage (Fig. 2(b)). The higher switching currents are also suppressed (Fig. 3) by the narrowing of the track, though by a smaller factor, and the high-bias conductivity is also reduced.

#### 4. Conclusions

We have shown experimentally that the switching current density is suppressed below the critical current density in intrinsic Josephson junction stacks with  $A < 1 \mu\text{m}^2$ . On the basis of our experimental data it is difficult to be conclusive about the mechanism for this suppression,

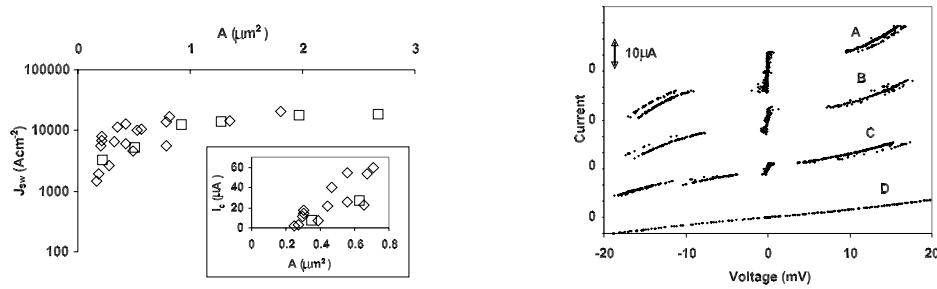


**Figure 2.**  $J_{SW}(A)$  (with a logarithmic axis) at 4.2 K for several intrinsic junction stacks. Diamonds represent the devices fabricated as described in this paper; squares represent devices on vicinal substrates (see [7]). The inset shows  $I_{SW}(A)$  (with a linear axis) for small junctions. (b) Two-point low- $T$  low-bias  $IV$  characteristics measured *in situ* in the FIB microscope. Labels indicate the extent of milling: A. before milling,  $w = 1.5 \mu\text{m}$ , B. after one milling stage, C. after two milling stages, D. after three milling stages,  $w = 0.5 \mu\text{m}$ . The plots are vertically offset from each other for clarity.

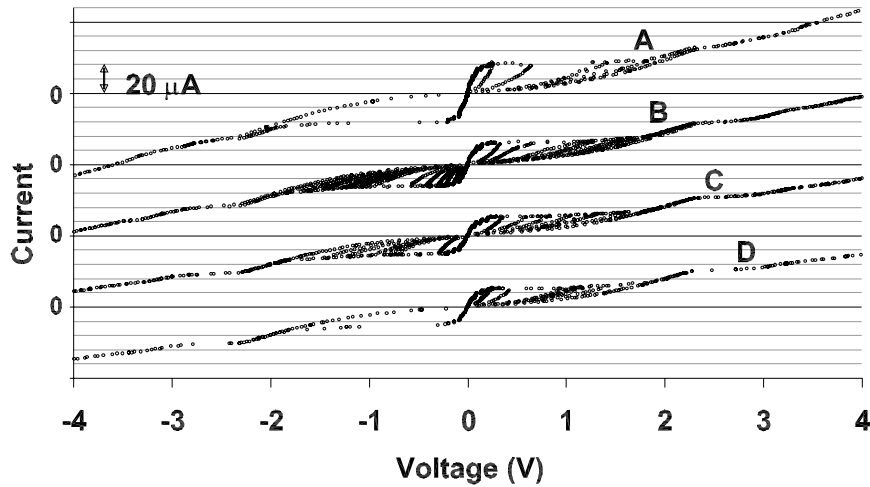


**Figure 3.** Two-point low- $T$   $IV$  characteristics measured *in situ* in the FIB microscope. Labels indicate the extent of narrowing (see Fig. 2(b) caption). Plots are offset vertically from each other for clarity.

though gallium ion-implantation and thermal fluctuations alone do not appear to account for it. To reach firmer conclusions about the relative importance of quantum fluctuations in these Josephson junction arrays, there is a need for sub- $\mu\text{m}^2$  junctions fabricated with greater control over  $N$ . We have also presented results using low- $T$  FIB milling with a liquid-helium-cooled stage and *in-situ* monitoring of the  $IV$  characteristics, a system which in future measurements will be employed to obtain this improved control.

### Acknowledgments

We would particularly like to acknowledge Gavin Burnell at the IRC in Nanotechnology at the University of Cambridge for the use of the Ar ion-beam miller there. We would also like to acknowledge fruitful input from Asan Kuzhakhmetov, Chris Bell, Mark Blamire and Henrik Schneidewind. This work is funded by the UK EPSRC.

- [1] R. Kleiner, F. Steinmeyer, G. Kunkel, and P. Müller. *Phys. Rev. Lett.*, 68:2394, 1992.
- [2] H.B. Wang, P.H. Wu, and T. Yamashita. *Phys. Rev. Lett.*, 87:107002, 2001.
- [3] J. Bylander, T. Duty, and P. Delsing. *Nature*, 434:361, 2005.
- [4] K.K. Likharev. *IEEE Trans. Mag.*, 25:1436, 1989.
- [5] K.K. Likharev and K.A. Matsuoka. *Appl. Phys. Lett.*, 67:3037, 1995.
- [6] S.J. Kim, Y.I. Latyshev, and T. Yamashita. *Appl. Phys. Lett.*, 74:1156, 1999.
- [7] P.A. Warburton, A.R. Kuzhakmetov, C. Bell, G. Burnell, M.G. Blamire, H. Wu, C.R.M. Grovenor, and H. Schneidewind. *IEEE Trans. Appl. Supercond.*, 13:821, 2003.
- [8] A.A. Yurgens, D. Winkler, N. Zavaritsky, and T. Claeson. *Appl. Phys. Lett.*, 70:1760, 1997.
- [9] P.A. Warburton, A.R. Kuzhakmetov, G. Burnell, M.G. Blamire, and H. Schneidewind. *Phys. Rev. B*, 67:184513, 2003.
- [10] P.A. Warburton, J.C. Fenton, M. Korsah, and C.R.M. Grovenor. Submitted to *Supercond. Sci. Tech.*
- [11] M. Tinkham. *Introduction to Superconductivity*. McGraw-Hill, New York, second edition, 1996.
- [12] V.M. Krasnov, T. Bauch, and P. Delsing. *Phys. Rev. B*, 72:012512, 2005.
- [13] Y.I. Latyshev and T. Yamashita. *J. Phys. IV*, 9:289, 1999.